



Elastostatic analysis using the boundary element method and the Aifantis gradient elasticity theory

Fabio C. da Rocha¹, Leslie D. P. Fernández², Julián B. Castellero³, Maria do S. M. Sampaio⁴

¹Graduate Program in Civil Engineering, Federal University of Sergipe
Av. Marcelo Deda Chagas, s/n, 49107-230, São Cristóvão - SE, Brazil
fabiocrocha@academico.ufs.br

²Dept. of Mathematics and Statistics, Federal University of Pelotas
Campus Universitário s/n, Prédio 5, 96160-000, Capão do Leão, Pelotas - RS, Brazil
leslie.fernandez@ufpel.edu.br

³IIMAS Academic Unit at Yucatan, National Autonomous University of Mexico
Tablaje Catastral 6998, Car. Mérida-Tetiz Km 4.5, 97357, Mérida, Mexico
julian@mym.iimas.unam.mx

⁴Dept. of Civil Engineering, Amazonas State University
Av. Djalma Batista, 3578, 69050-010, Manaus - AM, Brazil
msampaio@uea.edu.br

Abstract. The increasing use of micro and nanoscale structures has sparked interest in theories incorporating the effect of scale since the classical continuum theory has limitations in capturing effects that depend on size. With such a motivation, in this work, three-dimensional elastostatic microstructure modeling is carried out using the boundary element method (BEM). To account for microstructural effects, the simplified gradient theory proposed by Aifantis, a particularization of Mindlin's general theory, is employed. A variational argument is established to determine the governing equations and boundary conditions for the problem. This argument explains the fundamental solution of gradient elasticity, and the integral contour representation is constructed with the aid of the reciprocal identity. Curved triangular elements of Prorol spectral functions are used to approximate the geometry and the physical parameters for the BEM discretization. The presented formulation yields results consistent with other analyses in the literature.

Keywords: Aifantis gradient elasticity theory, Boundary element method, Prorol spectral functions

1 Introduction

The theory of classical continuous medium mechanics, including linear and non-linear elasticity, damage, and plasticity, has been widely used in applications in civil, chemical, electrical, and mechanical engineering and several other fields of physics and life sciences. This theory was initially developed to describe deformation phenomena and processes that can be observed with the naked eye, that is, problems on scales ranging from millimeters to meters. However, in the last century, it was used to describe phenomena ranging from atomistic to terrestrial scales (faults and earthquakes) (Askes and Aifantis [1]). It is in the micro- and nano-scale regime that the dimensions of the structure become comparable to the size of the material's microstructure, and both microstructural and size effects cannot be neglected. Examples of the importance of the size effect are significant in the analysis of thin films and plates, micro-beams, microelectronic and micromechanical devices, as well as in the phenomenon of wave propagation in materials, such as polycrystals, polymers, bones, and reinforced composites by fibers or particles (Polyzos and Fotiadis [2], Lei et al. [3], Aifantis [4]).

Due to the lack of internal length scale parameters, the classical theory of elasticity fails to describe the behavior of materials on the micro and nanoscale. However, it is possible to overcome this deficiency through so-called improved elastic theories, in which the intrinsic parameters that correlate the microstructure with the macrostructure are involved in the constitutive equations and the equation of motion of the elastic continuum. Among the improved theories, there is the gradient strain theory (Toupin [5]) and the high-order elastic gradient strain theory (Mindlin [6]).

With the increased use of computational methods, the implementation of gradient elasticity has become the

focus of some studies, especially in the application of the boundary element method (BEM), as it is non-trivial due to the complexity of partial differential equations that govern the problems and the fundamental solution that the method requires. However, BEM has the advantage of reducing the dimensionality of the problems and the absence of the need for C^1 -continuity of the approximating functions, which makes this numerical method ideal for analyzing elastic gradient problems (Beskos [7, 8]).

The present work aims to employ and analyze the precision of the approximating function of any order formed by Proriol polynomials (Blyth and Pozrikidis [9]) and interpolated, at strategically allocated points, in the positions of the zeros of the Lobatto polynomials after symmetrization through a mapping in the domain of the triangular element. The work is presented as follows: in section 2, the constitutive equations and boundary conditions are given; in section 3, the fundamental 3D solution for gradient elastostatic problems is presented; in section 4, the integral identity and integral contour representation are shown; in section 5, the formulation of the BEM is presented; in section 6 the Proriol approximation base is described; in section 7 the process of obtaining the Lobatto nodal distribution for a triangular element is shown; and in section 8 an example of validation is presented.

2 Governing equations, boundary conditions, and constitutive model

Some notations used require a presentation. The first refers to the vertical double and triple dot operation to represent the double and triple contraction inner products, respectively, which obey the rules:

$$(a \otimes b) : (c \otimes d) = (b \cdot c) (a \cdot d),$$

$$(a \otimes b \otimes m) \dot{ : } (I \otimes c \otimes d) = (m \cdot I) (b \cdot c) (a \cdot d), \quad (1)$$

where a, b, c, d, m, I are vectors in three-dimensional space and \otimes represents the tensor product. The symbol $(\circ)^{321}$ is defined as

$$(a \otimes b \otimes c)^{321} = (c \otimes b \otimes a). \quad (2)$$

Let a linear elastic body of volume V be limited by the surface S . The geometry of this body is described with the help of the unit normal vector \hat{n} in S , referenced in a Cartesian coordinate system with the origin located inside V . According to Lam et al. [10] and Rocha [11], in which the macroscopic strain tensor was considered equal to that of the micro-configuration, the internal strain energy is described by eq.(3),

$$\begin{aligned} \delta \mathfrak{N} = & - \int_V [\nabla \cdot (\tilde{\tau} - \nabla \cdot \tilde{\mu}) \cdot \delta \bar{u}] dV + \int_S (\hat{n} \cdot \tilde{\mu} \cdot \hat{n}) [\hat{n} \cdot \nabla (\delta \bar{u})] dS + \\ & \int_S \{ \hat{n} \cdot \tilde{\tau} - (\hat{n} \otimes \hat{n}) : \frac{\partial \tilde{\mu}}{\partial n} - \hat{n} \cdot (\nabla_S \cdot \tilde{\mu}) - \hat{n} \cdot [\nabla_S \cdot (\tilde{\mu})^{213}] \} \cdot \delta \bar{u} dS + \\ & \int_S [(\nabla_S \cdot \hat{n})(\hat{n} \otimes \hat{n}) : \tilde{\mu} - (\nabla_S \hat{n}) : \tilde{\mu}] \cdot \delta \bar{u} dS + \sum_{C_a} \oint_{C_a} \{ \|(\hat{m} \otimes \hat{n}) : \tilde{\mu}\| \cdot \delta \bar{u} \} dC, \end{aligned} \quad (3)$$

where C_a are the contours formed by the intersection of two surface portions S_1 and S_2 of S . Also, $\tilde{\tau}$ is the symmetric stress tensor, \bar{u} is the displacement vector, ∇ is the gradient operator, $\nabla_S (= (\tilde{I} - \hat{n} \otimes \hat{n}) \cdot \nabla)$ is the surface gradient operator, \tilde{I} denoting the unit tensor, $\tilde{\mu}$ is the double forces per unit area, with 27 components μ_{ijk} . In addition, \hat{m} is the outer conormal vector that satisfies $\hat{m} = \hat{s} \times \hat{n}$, with \hat{s} being the unit tangent vector to C_a .

The variation of the work done by external forces in V is due to the body force \mathbf{f} , the external surface tractions \mathbf{P} , the surface double stresses \mathbf{R} and the surface jump stresses \mathbf{E} . Thus, the variational equation of external work done can be written as (Mindlin [6])

$$\delta \mathfrak{N}_1 = \int_V \mathbf{f} \cdot \delta \bar{u} dV + \int_S \mathbf{R} \cdot [\hat{n} \cdot \nabla (\delta \bar{u})] dS + \int_S \mathbf{P} \cdot \delta \bar{u} dS + \sum_{C_a} \oint_{C_a} (\mathbf{E} \cdot \delta \bar{u}) dC. \quad (4)$$

Based on the fact that $\delta \mathfrak{N} = \delta \mathfrak{N}_1$, and relating eq.(3) with eq.(4), the equilibrium for two- and three-dimensional gradient elastic bodies can be described by the equation:

$$\nabla \cdot (\tilde{\tau} - \nabla \cdot \tilde{\mu}) + \mathbf{f} = 0. \quad (5)$$

The boundary conditions for traction and displacement, present in the classical formulation of elasticity but with the incorporation of microstructure, are, respectively:

$$\mathbf{P} = \hat{n} \cdot \tilde{\tau} - (\hat{n} \otimes \hat{n}) : \frac{\partial \tilde{\mu}}{\partial n} - \hat{n} \cdot (\nabla_S \cdot \tilde{\mu}) - \hat{n} \cdot [\nabla_S \cdot (\tilde{\mu})^{213}] + (\nabla_S \cdot \hat{n})(\hat{n} \otimes \hat{n}) : \tilde{\mu} - (\nabla_S \hat{n}) : \tilde{\mu} = \mathbf{P}_0, \quad (6)$$

$$\bar{u} = \bar{u}_0, \quad (7)$$

and the additional *non-classical* boundary conditions

$$\mathbf{R} = \hat{n} \cdot \tilde{\mu} \cdot \hat{n} = \mathbf{R}_0, \quad (8)$$

$$\mathbf{E} = \|(\hat{m} \otimes \hat{n}) : \tilde{\mu}\| = \mathbf{E}_0, \quad (9)$$

where \mathbf{P}_0 , \bar{u}_0 , \mathbf{R}_0 , \mathbf{q}_0 and \mathbf{E}_0 represent prescribed values. Making use of the considerations for isotropic material adopted in Mindlin [6], the constitutive equations are expressed by

$$\begin{aligned} \tilde{\sigma} &= \tilde{\tau} + \tilde{s}, \quad \tilde{\tau} = 2\mu\tilde{\varepsilon} + \lambda(\nabla \cdot \bar{u})\tilde{I}, \quad \tilde{\varepsilon} = \frac{(\nabla\bar{u} + \bar{u}\nabla)}{2}, \\ \tilde{s} &= -[2\mu c_3 \nabla^2 \tilde{\varepsilon} + \lambda c_1 \tilde{I} \nabla^2 (\nabla \cdot \bar{u}) + \lambda c_2 \nabla \nabla (\nabla \cdot \bar{u})], \end{aligned} \quad (10)$$

where ∇^2 is the Laplacian operator, $\tilde{\varepsilon}$ is the strain tensor, $\tilde{\sigma}$ is the total stress tensor, $\tilde{\tau}$ and \tilde{s} are called Cauchy stress tensor and relative stress tensor, respectively. The total stress tensor is correlated to the strain tensor and the gradient of the strain tensor through five independent material constants (λ , μ , c_1 , c_2 and c_3), the first two of which are known as the Lamé constant (Mindlin [6]).

The simplest and mathematically least difficult-to-manipulate constitutive equation is proposed by Aifantis and co-authors (Aifantis [12], Ru and Aifantis [13]), in which they correlate the double stress tensor, $\tilde{\mu}$, with the relative stress tensor, \tilde{s} , according to the relations:

$$\tilde{\mu} = g^2 \nabla \tilde{\tau}, \quad \tilde{s} = -\nabla \cdot \tilde{\mu} = -g^2 \nabla \cdot \nabla \tilde{\tau} = -g^2 \nabla^2 \tilde{\tau}, \quad (11)$$

where g^2 is the only parameter that links the microstructure to the microstructure, known as the characteristic length. Adopting the simplifications of Aifantis' theory and substituting eq.(11) into eq.(5), we obtain the equation of motion for gradient elasticity of the continuous medium in terms of the displacement field \bar{u} :

$$\mu \nabla^2 \bar{u} + (\lambda + \mu) \nabla \nabla \cdot \bar{u} - g^2 \nabla^2 [\mu \nabla^2 \bar{u} + (\lambda + \mu) \nabla \nabla \cdot \bar{u}] + f = 0. \quad (12)$$

3 Fundamental solution

This section presents the fundamental three-dimensional solution for gradient elastostatic problems. This solution is defined as a particular solution of the following partial differential equation

$$L\tilde{u}^*(r) = -\Delta(y-x)\tilde{I}, \quad (13)$$

where Δ is the Dirac delta function, y is the displacement field point, $L\tilde{u}^*(r) = -\Delta(y-x)\tilde{I}$, due to the unitary force applied at point x . Also, r is the distance between the field point and the source point ($r = |y-x|$), and L is the linear operator

$$L \equiv \mu \nabla^2 + (\lambda + \mu) \nabla \nabla \cdot - g^2 \nabla^2 [\mu \nabla^2 + (\lambda + \mu) \nabla \nabla \cdot]. \quad (14)$$

The fundamental solution of eq. (13) is given by (Rocha [11])

$$\tilde{u}^*(r, \mu, \nu, g) = \frac{1}{16\pi\mu(1-\nu)} [\Upsilon(r, \nu, g)\tilde{I} - \chi(r, g)\hat{r} \otimes \hat{r}], \quad (15)$$

where ν is the Poisson ratio, \hat{r} is the unit vector of the radius \mathbf{r} and, finally, Υ and χ are scalar functions given by :

$$\begin{aligned} \Upsilon(r, \nu, g) &= (3-4\nu)\frac{1}{r} + 2(1-2\nu) \left[-\frac{g^2}{r^3} + \left(\frac{g^2}{r^3} + \frac{g}{r^2} \right) e^{-r/g} \right] + \\ &4(1-\nu) \left[-\frac{g^2}{r^3} + \left(\frac{g^2}{r^3} + \frac{g}{r^2} + \frac{1}{r} \right) e^{-r/g} \right], \end{aligned} \quad (16)$$

$$\chi(r, g) = -\frac{1}{r} + \frac{6g^2}{r^3} - \left(\frac{6g^2}{r^3} + \frac{6g}{r^2} + \frac{2}{r} \right) e^{-r/g}, \quad (17)$$

for three-dimensional problems.

4 Integral identity and integral boundary representation

The valid reciprocal identity for the gradient elasticity presented in this work can be written, for non-smooth surface S , as (Polyzos et al. [14])

$$\begin{aligned} & \int_V \{\mathbf{f}^* \cdot \bar{u} - \mathbf{f} \cdot \bar{u}^*\} dV + \int_S \{\mathbf{P}^* \cdot \bar{u} - \mathbf{P} \cdot \bar{u}^*\} dS \\ &= \int_S \left\{ \mathbf{R} \cdot \frac{\partial \bar{u}^*}{\partial n} - \mathbf{R}^* \cdot \frac{\partial \bar{u}}{\partial n} \right\} dS + \sum_{C_a} \oint_{C_a} (\mathbf{E} \cdot \bar{u}^* - \mathbf{E}^* \cdot \bar{u}) dC. \end{aligned} \quad (18)$$

If the surface S is smooth, the last integral of eq.(18) becomes zero. It is assumed that the displacement field \bar{u}^* is the result of an excitation in the state of deformation and tension $(\bar{u}^*, \bar{\sigma}^*)$, in the form:

$$f^* = \Delta(y - x)\hat{e}, \quad (19)$$

with \hat{e} being the direction of the unit force acting at point x . The fields $\bar{u}^*(y)$, $P^*(y)$, $R^*(y)$ and $E^*(y)$ can be represented, respectively, by the fundamental tensors $\tilde{u}^*(x, y)$, $\tilde{P}^*(x, y)$, $\tilde{R}^*(x, y)$ and $\tilde{E}^*(x, y)$, according to the following relations

$$\bar{u}^*(y) = \tilde{u}^*(x, y) \cdot \hat{e}, \quad P^*(y) = \tilde{P}^*(x, y) \cdot \hat{e}, \quad R^*(y) = \tilde{R}^*(x, y) \cdot \hat{e}, \quad E^*(y) = \tilde{E}^*(x, y) \cdot \hat{e}. \quad (20)$$

Applying eq.(15) and eq.(20) to eqs.(6) - (9), the fundamental solutions \mathbf{P}^* , \mathbf{R}^* and \mathbf{E}^* are obtained. Substituting eq.(20) in eq.(18) and using the symmetry of the fundamental solution \tilde{u}^* , the following boundary integral equation is obtained

$$\begin{aligned} & \tilde{c}(x) \cdot \bar{u}(x) + \int_S \left\{ \tilde{\mathbf{P}}^*(x, y_b) \cdot \bar{u}(y_b) - \tilde{\mathbf{U}}^*(x, y_b) \cdot P(y_b) \right\} dS_{y_b} \\ &= \int_S \left[\tilde{\mathbf{Q}}^*(x, y_b) \cdot R(y_b) - \tilde{\mathbf{R}}^*(x, y_b) \cdot q(y_b) \right] dS_{y_b} + \\ & \sum_{C_a} \oint_{C_a} \left(\tilde{\mathbf{U}}^*(x, y_b) \cdot E(y_b) - \tilde{\mathbf{E}}^*(x, y_b) \cdot \bar{u}(y_b) \right) dC_{y_b} + \int_V \left[\tilde{\mathbf{U}}^*(x, y) \cdot f(y) \right] dV, \end{aligned} \quad (21)$$

where y_b represents the field point on the contour, $q = \partial \bar{u}(y_b) / \partial n_{y_b}$, $\tilde{\mathbf{U}}^* = \tilde{u}^*$, $\tilde{\mathbf{P}}^* = (\tilde{\mathbf{P}}^*)^T$, $\tilde{\mathbf{Q}}^* = (\partial \tilde{u}^* / \partial n_{y_b})^T$, $\tilde{\mathbf{R}}^* = (\tilde{\mathbf{R}}^*)^T$, $\tilde{\mathbf{E}}^* = (\tilde{\mathbf{E}}^*)^T$ and the jump tensor $\tilde{c}(x)$ is given by (Brebbia and Dominguez [15])

$$\tilde{c}(x) = 0, \text{ if } x \in (R^3 - V), \quad \tilde{c}(x) = \tilde{I}, \text{ if } x \in V, \quad \tilde{c}(x) = \frac{1}{2}\tilde{I}, \text{ if } x \in S. \quad (22)$$

Equation (21) has five field unknowns (considering the absence of body force), that is, $\bar{u}(y_b)$, $P(y_b)$, $q(y_b)$, $R(y_b)$ and $E(y_b)$. There are also three boundary conditions, and an additional integral equation needs to be incorporated to obtain all field unknowns. This additional equation is obtained by applying the differential operator $\partial / \partial n_x$ to eq. (21) and disregarding the body force.

5 Boundary element method for gradient elastic body

For the BEM implementation in FORTRAN, the smooth surface S is discretized into E triangular boundary elements. For a nodal point k , the eq. (18) and its partial derivative concerning the normal have, respectively, the form:

$$\frac{1}{2}\bar{u}^k + \sum_{\beta=1}^{\tilde{L}} H_{\beta}^k \cdot u^{\beta} + \sum_{\beta=1}^{\tilde{L}} K_{\beta}^k \cdot q^{\beta} = \sum_{\beta=1}^{\tilde{L}} G_{\beta}^k \cdot P^{\beta} + \sum_{\beta=1}^{\tilde{L}} L_{\beta}^k \cdot R^{\beta}, \quad (23)$$

$$\frac{1}{2}q^k + \sum_{\beta=1}^{\tilde{L}} S_{\beta}^k \cdot u^{\beta} + \sum_{\beta=1}^{\tilde{L}} T_{\beta}^k \cdot q^{\beta} = \sum_{\beta=1}^{\tilde{L}} V_{\beta}^k \cdot P^{\beta} + \sum_{\beta=1}^{\tilde{L}} W_{\beta}^k \cdot R^{\beta}. \quad (24)$$

With $\bar{u}^k = \bar{u}(x^k)$, $q^k = q(x^k) = \frac{\partial \bar{u}(x^k)}{\partial n_x}$, \tilde{L} being the total number of nodes, β the global numbering for the nodes, which is associated with each pair (e, a) . e and a represent the element and node number, respectively. Additionally, there is

$$A_{\beta}^k = \int_{-1}^1 \int_{-1}^1 B(x^k, y(\xi_1, \xi_2)) N^a(\xi_1, \xi_2) J(\xi_1, \xi_2) d\xi_1 d\xi_2, \quad (25)$$

where if $A = H \Rightarrow B = \tilde{P}^*$, or $A = K \Rightarrow B = \tilde{R}^*$, or $A = G \Rightarrow B = \tilde{U}^*$, or $A = L \Rightarrow B = \tilde{Q}^*$, or $A = S \Rightarrow B = \frac{\partial \tilde{P}^*}{\partial n_x}$, or $A = T \Rightarrow B = \frac{\partial \tilde{R}^*}{\partial n_x}$, or $A = V \Rightarrow B = \frac{\partial \tilde{U}^*}{\partial n_x}$, or $A = W \Rightarrow B = \frac{\partial \tilde{Q}^*}{\partial n_x}$. N^a is also defined as the shape functions of a triangular element, J the Jacobian of the transformation of the global coordinate system (X_1, X_2, X_3) for dimensionless local (ξ_1, ξ_2) and, finally, $u^\beta, q^\beta, P^\beta, R^\beta$ are the nodal values of the corresponding field functions.

6 Prorior polynomial base

Prorior polynomials are the base of interest in this work, as they are entirely orthogonal over the triangle area (Prorior [16]). To introduce this polynomial base, the standard triangle is initially mapped from the plane $\xi_1 - \xi_2$ to the standard square $-1 \leq \xi'_1 \leq 1, -1 \leq \xi'_2 \leq 1$, using the Duffy transformation:

$$\xi_1 = \frac{(1 + \xi'_1)(1 - \xi'_2)}{4}, \quad \xi_2 = \frac{(1 + \xi'_2)}{2}. \quad (26)$$

Prorior polynomials (Prorior [16]) is formed by the product of Legendre and Jacobi polynomials, whose explicit expression is given by

$$PR_{kl} = \left[\sum_{i=0}^k \left(\frac{k!}{i!(k-i)!} \right)^2 \left(\frac{\xi'_1 - 1}{2} \right)^{k-i} \left(\frac{\xi'_1 + 1}{2} \right)^i \right] \left(\frac{1 - \xi'_2}{2} \right)^k \times \left[\sum_{j=0}^l \frac{(l + 2k + 1)!}{j!(l + 2k + 1 - j)!} \frac{l!}{(l - j)!j!} \left(\frac{\xi'_2 - 1}{2} \right)^{l-j} \left(\frac{\xi'_2 + 1}{2} \right)^j \right]. \quad (27)$$

7 Lobatto nodal distribution for triangular element

Once Lobatto's nodal distribution is known to be optimal for one-dimensional interpolation (Pozrikidis [17]), this work is motivated to use the one-dimensional nodal distribution with $v_1 = 0, v_{m+1} = 1$ and the nodes inside $v_i, i = 2, 3, \dots, m$, positioned at the scaled zeros of the polynomial of Lobatto grade $m - 1$. Thus, Lobatto's nodal distribution is defined by:

$$v_1 = 0, \quad v_i = \frac{1}{2}(1 - t_{i-1}) \quad \text{and} \quad v_{m+1} = 1, \quad (28)$$

where t_i , for $i = 2, 3, \dots, m$, are the zeros of the Lobatto polynomial of degree $m - 1$ distributed in the open interval $(-1, 1)$. The i -th term of the Lobatto polynomial is defined as $Lo_i(t) \equiv L'_{i+2}(t)$, where $L'_{i+2}(t)$ is the first derivative of the Legendre polynomial. The nodes on the contour and inside are identified by the coordinates $(\xi_1, \xi_2) = (v_i, v_j)$, where $i = 1, \dots, m + 1$ and $j = 1, \dots, m + 2 - i$. The nodes are redistributed using the mapping specified by Blyth and Pozrikidis [9] and described by eq. (29) to ensure a symmetrical distribution of nodes around the three vertices:

$$\xi_1^i = \frac{1}{3}(1 + 2v_j - v_i - v_k), \quad \xi_2^j = \frac{1}{3}(1 + 2v_j - v_i - v_k), \quad (29)$$

with $i = 1, 2, \dots, m + 1, j = 1, 2, \dots, m + 2 - i$ e $k = m + 3 - i - j$.

8 Validation example

Let there be a spherical solid of radius a and subjected to a radial displacement u_0 (classical boundary condition), while the normal displacement gradient is zero at the boundary (non-classical boundary condition), that is,

$$\mathbf{u}(r)|_{r=a} = u_0 \hat{\mathbf{r}}, \quad (30)$$

$$\mathbf{q}_r(r)|_{r=a} = \frac{\partial \mathbf{u}_r(r)}{\partial n} \Big|_{r=a} = 0, \quad (31)$$

where $\mathbf{u}(r)$ is the radial displacement and r the distance from the center of the sphere. The analytical displacement solution for this problem is presented in Tsepoura et al. [18]. This problem is solved numerically by formulating

the micromechanical BEM considering the Proriol approximation of degree 4 and compared with both analytical and numerical results presented in Tsepoura et al. [18]. This example adopted the following values: $u_0 = 1$, $a = 1$ and $\nu = 0$. The problem was discretized by 256 triangular elements for the approach via BEM - Proriol degree 4, while Tsepoura et al. [18] used 304 quadrilateral quadratic elements. This new approach has proven to be convergent and stable, even at higher-order degrees, such as fourth-order. Figs.(1-2) show, respectively, the values of the radial displacement u_r , strain ε_r , double stress μ_{rrr} and total stress σ_{rr} as the value of the characteristic length g is varied. The results show good agreement between the proposed formulation and the numerical and analytical results presented in Tsepoura et al. [18], with errors of less than 1.5%. In Fig. 2-b, only the results of the BEM - Proriol formulation and the analytical solution are presented since Tsepoura et al. [18] does not present numerical results for the total stress. When g is small, deformation gradient theory is less necessary. However, as g increases, gradient theories become crucial for accurate mechanical analysis, such as in small-scale problems.

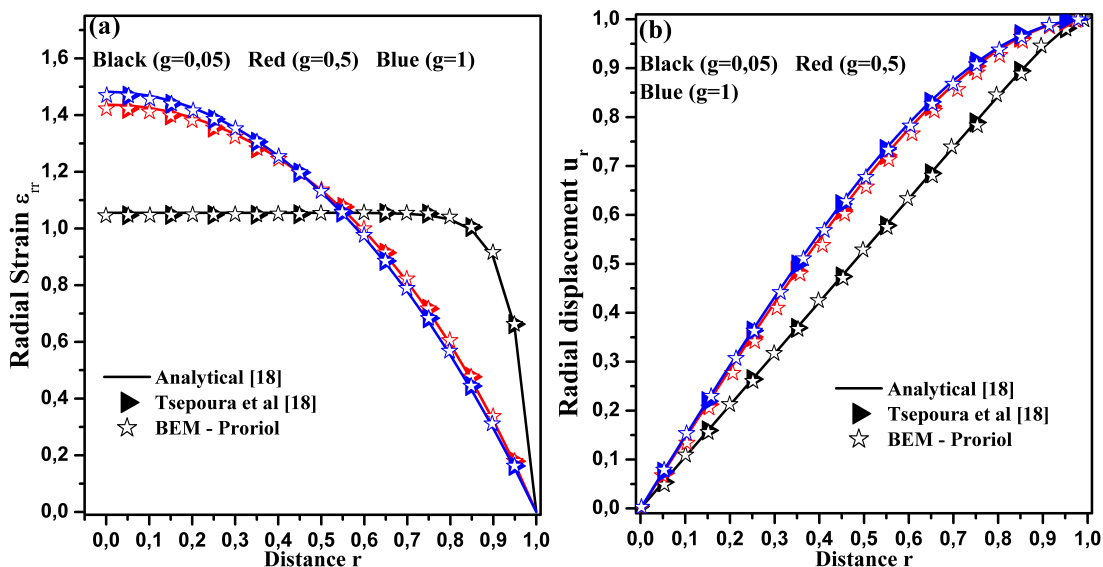


Figure 1. Behaviors of strain (a) and displacement (b), both in the radial direction, as the parameter g varies. The solid line and the triangle and star markers represent, respectively, the analytical solution, that of Tsepoura et al. [18] and the present model.

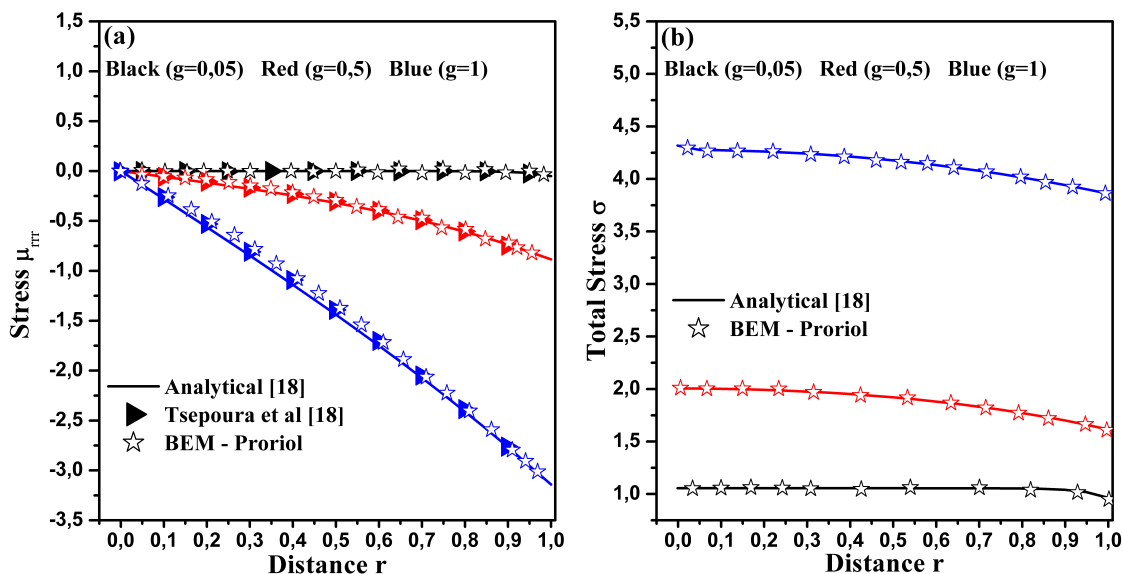


Figure 2. Behaviors of double stress (a) and total stress (b), both in the radial direction, as the parameter g varies. The solid line and the triangle and star markers represent, respectively, the analytical solution, that of Tsepoura et al. [18] and the present model.

9 Conclusions

This work develops and implements a BEM formulation, considering microstructural effects in three-dimensional elastostatic problems. The simplified elastic gradient theory of Aifantis, a particularization of Mindlin's general theory, was used to consider the microstructural effect. To formulate the BEM, triangular elements of any order from Proriol were interpolated at the Lobatto polynomials' zero nodes to construct the shape functions. The BEM-Proriol-Lobatto coupling proved efficient and convergent to the reference results without losing precision and without the Runge effect.

Acknowledgements. The authors thank CNPq for financial support (Universal Project No. 402857/2021-6). FCR, LDPF, and JBC also thank FAPITEC (Universal Project No. 019203.01702/2024-6), with FCR extending thanks to the FAPITEC/SE/FUNTEC Call No. 02/2024.

Authorship statement. The authors hereby confirm that they are the sole liable persons responsible for the authorship of this work, and that all material that has been herein included as part of the present paper is either the property (and authorship) of the authors, or has the permission of the owners to be included here.

References

- [1] H. Askes and E. Aifantis. Gradient elasticity in statics and dynamics: An overview of formulations, length scale identification procedures, finite element implementations and new results. *International Journal of Solids and Structures*, vol. 48, pp. 1962–1990, 2011.
- [2] D. Polyzos and D. Fotiadis. Derivation of mindlin's first and second strain gradient elastic theory via simple lattice and continuum models. *International Journal of Solids and Structures*, vol. 49, pp. 470–480, 2012.
- [3] J. Lei, P. Ding, and C. Zhang. Boundary element analysis of static plane problems in size-dependent consistent couple stress elasticity. *Engineering Analysis with Boundary Elements*, vol. 132, pp. 399–415, 2021.
- [4] E. C. Aifantis. A concise review of gradient models in mechanics and physics. *Frontier in Physics*, vol. 7, pp. 1–8, 2020.
- [5] R. Toupin. Theories of elasticity with couple-stress. *Archive for Rational Mechanics and Analysis*, vol. 17, pp. 85–112, 1964.
- [6] R. D. Mindlin. Micro-structure in linear elasticity. *Archive for Rational Mechanics and Analysis*, vol. 16, n. 1, pp. 51–78, 1964.
- [7] D. Beskos. Boundary element methods in dynamic analysis. *Applied Mechanics Reviews*, vol. 40, pp. 1–23, 1987.
- [8] D. Beskos. Boundary element methods in dynamic analysis. part ii. *Applied Mechanics Reviews*, vol. 50, pp. 149–197, 1997.
- [9] M. Blyth and C. Pozrikidis. A lobatto interpolation grid over triangle. *IMA Journal of Applied Mathematics*, vol. 71, pp. 153–169, 2005.
- [10] D. Lam, F. Yang, A. Chong, J. Wang, and P. Tong. Experiments and theory in strain gradient elasticity. *Journal of the Mechanics and physics of Solids*, vol. 51, n. 8, pp. 1477–1508, 2003.
- [11] F. C. D. Rocha. *Formulation of the BEM Considering Microstructural Effects and G1 Geometric Continuity: Singularity Treatment and Convergence Analysis*. EESC/USP, 2015.
- [12] E. Aifantis. On the role of gradient in the localization of deformation and fracture. *International journal of Engineering Science*, vol. 30, pp. 1279–1299, 1992.
- [13] V. Ru and E. Aifantis. A simple approach to solve boundary value problems in gradient elasticity. *Acta Mechanica*, vol. 101, pp. 59–68, 1993.
- [14] D. Polyzos, K. Tsepoura, S. Rsinopoulos, and D. Beskos. A boundary element method for solving 2-d and 3-d static gradient elastic problems: Part i: Integral formulation. *Computer Methods in Applied Mechanics and Engineering*, vol. 192, n. 26-27, pp. 2845–2873, 2003.
- [15] C. Brebbia and J. Dominguez. *Boundary Element Method: An introductory course*. WIT Press, 1992.
- [16] J. Proriol. Sur une famille de polynomes à deux variables orthogonaux dans un triangle. *Comptes Rendus de l'Académie des Sciences*, vol. 245, pp. 2459–2461, 1957.
- [17] C. Pozrikidis. *Introduction to Finite and Spectral Element Methods using MATLAB*. Chapman and Hall/CRC, 2005.
- [18] K. Tsepoura, S. Tsinopoulos, D. Polyzos, and D. Beskos. A boundary element method for solving 2-d and 3-d static gradient elastic problems part ii: Numerical implementation. *Computer Method in Applied Mechanics and Engineering*, vol. 192, n. 26-27, pp. 2875–2907, 2003.